Published in final edited form as:
J Med Chem. 2008 December 25; 51(24): 8012–8018. doi:10.1021/jm801142b.

Examining the Chirality, Conformation and Selective Kinase Inhibition of 3-((3*R*,4*R*)-4-methyl-3-(methyl(7H-pyrrolo[2,3-d]pyrimidin-4-yl)amino)piperidin-1-yl)-3-oxopropanenitrile (CP-690,550)

Jian-kang Jiang[a], **Kamran Ghoreschi**[b], **Francesca Deflorian**[c], **Zhi Chen**[b], **Melissa Perreira**[a], **Marko Pesu**[b], **Jeremy Smith**[a], **Dac-Trung Nguyen**[a], **Eric H. Liu**[d], **William Leister**[a], **Stefano Costanzi**[c], **John J. O'Shea**[b], and **Craig J. Thomas**[a,*]

a*NIH Chemical Genomics Center, National Human Genome Research Institute, National Institutes of Health, 9800 Medical Center Drive, Rockville, Maryland 20850, USA*

b*Molecular Immunology and Inflammation Branch, National Institute of Arthritis and Musculoskelatal and Skin Diseases, National Institutes of Health, Bethesda, Maryland 20850, USA*

c*Laboratory of Biological Modeling, National Institute of Diabetes and Digestive and Kidney Diseases, NIH, Bethesda, MD 20892, USA*

d*Transplantation and Autoimmunity Branch, National Institute of Diabetes and Digestive and Kidney Diseases, NIH, Bethesda, MD 20892, USA*

Abstract

Here, we examine the significance that stereochemistry plays within the clinically relevant Janus Kinase 3 (Jak3) inhibitor CP-690,550. A synthesis of all four enantiopure stereoisomers of the drug was carried out and an examination of each compound revealed that only the enantiopure 3*R*, 4*R* isomer was capable of blocking Stat5 phosphorylation (Jak3 dependent). Each compound was profiled across a panel of over 350 kinases which revealed a high level of selectivity for the Jak family kinases for these related compounds. Each stereoisomer retained a degree of binding to Jak3 and Jak2 and the 3*R*, 4*S* and 3*S*, 4*R* stereoisomers were further revealed to have binding affinity for selected members of the STE7 and STE20 subfamily of kinases. Finally, an appraisal of the minimum energy conformation of each stereoisomer and molecular docking at Jak3 was performed in an effort to better understand each compounds selectivity and potency profiles.

Keywords

Janus Kinase 3; CP-690,550; Kinase inhibition; Chiral drugs

Introduction

The potent and selective Janus Kinase 3 (Jak3) inhibitor CP-690,550 (3-((3*R*,4*R*)-4-methyl-3-(methyl(7H-pyrrolo[2,3-d]pyrimidin-4-yl)amino)piperidin-1-yl)-3-oxopropanenitrile) (**1**)

Send proofs to: Dr. Craig J. Thomas, NIH Chemical Genomics Center, NHGRI, National Institutes of Health, 9800 Medical Center Drive, Building B, Room 3005, MSC: 3370, Bethesda, MD 20892-3370, 301-217-4079, 301-217-5736 (fax), craigt@nhgri.nih.gov.

Supporting Information Available: Synthetic procedures, selected spectra, expanded experiments and complete profile results. This material is available free of charge via the Internet.

was reported in 2003 as an orally active immunosuppressant for autoimmune disease and transplant patients.[1] The structure was revealed as a substituted piperidine linked to a deazapurine core (**1**) (Figure 1). Interestingly, the initial report did not designate the stereochemistry at the 3 and 4 positions of the substituted piperidine ring. Reports within the patent literature[2-4] and subsequent manuscripts[5,6] have denoted the structure as the enantiopure (3*R*, 4*R*) analogue **1**. At the time of writing, **1** has demonstrated efficacy in phase 2 clinical evaluation as an immunosuppressive for renal transplant rejection [7] and for treatment of rheumatoid arthritis.[8] Undoubtedly, a major foundation for the clinical success of this agent is the potent and selective Jak3 inhibition. The original report provided evidence that **1** inhibited Jak3 with an IC_{50} value of 1 nM while inhibiting Jak2, Jak1, Rock-II and Lck with IC_{50} values of 20 nM, 112 nM, 3,400 nM and 3,870 nM, respectively.[1] A panel of 28 other kinases did not demonstrate any relevant inhibition. Recently, Karaman et al. presented the interaction maps for 38 clinically relevant kinase inhibitors across a panel of 317 kinases.[9] The manuscript included **1** and reported the binding potential at Jak3 and Jak2 as 2.2 nM and 5 nM (Kd) [the primary kinase domain of Jak1 was not incorporated in this screen]. The report included additional binding for **1** at Camk1 (Kd of 5,000 nM), DCamkL3 (Kd of 4.5 nM), Mst2 (Kd of 4,300 nM), Pkn1 (Kd of 200 nM), Rps6ka2 (Kin.Dom.2 – C-terminal) (Kd of 1,400 nM), Rps6ka6 (Kin.Dom.2 – C-terminal) (Kd of 1,200 nM), Snark (Kd of 420 nM), Tnk1 (Kd of 640 nM) and Tyk2 (Kd of 620 nM).

Despite these additional activities, **1** remains a remarkably selective kinase inhibitor. In a recent report, Changelian et al. related the clinical success of Jak3 inhibitors directly to their selectivity.[10] As the binding of any small molecule to a protein target is inextricably linked to its structure, we found the stereospecific nature of **1** and its selectivity against over 300 kinases to be of interest. Hoping to explore this facet of the molecule we first set out to synthesize **1** and its three related stereoisomeric derivatives (analogues **2**, **3** and **4**) (Figure 1).

Results

Synthesis of 1, 2, 3 and 4

The synthetic route undertaken by Pfizer has evolved to ultimately rely upon a 4-step transformation yielding the requisite (3*R*,4*R*)-1-benzyl-*N*,4-dimethylpiperidin-3-amine from 4-methylpyridin-3-amine (Scheme 1).[5] Crystallization with a di-*p*-toluoyltartrate salt was utilized to achieve enantiopurity following reduction of the substituted pyridine derivative. This route provides an elegant and efficient means to yield kilograms of the enantiomerically pure material needed for efficient production of **1**. It does not, however, provide a means to investigate 3,4-*trans* analogues of the piperidine ring. To explore the desired alternate stereochemical possibilities we expanded upon a method described by Ledoussal and coworkers that relies upon the stereocenter that is set within Garner's aldehyde and a key step involving the ring-closing metathesis reaction (Scheme 2).[11] Here, the ultimate stereocenter at C3 of the piperidine ring is set by the choice of L-serine and utilizes precedented chemistry[12] to arrive at (*R*)-tert-butyl 2,2-dimethyl-4-(prop-1-en-2-yl)oxazolidine-3-carboxylate (**6**) (see supporting information for full synthetic details). Although several deviations from the reported work by Ledoussal and coworkers[11] were necessary, the general strategy provided (*R*)-*tert*-butyl 1-(allyl(benzyl)amino)-3-methylbut-3-en-2-ylcarbamate (**7**) in good yields. Application of the Grubbs 2nd generation catalyst in refluxing dichloromethane afforded the requisite piperidine derivative **8** in yields typically exceeding 90%. Hydrogenation of the 3,4-alkene moiety resulted in the chromatographically separable piperidines **9** and **10**. Following separation, the remainder of the synthesis followed the synthetic strategy validated by White and coworkers to arrive at both **1** and **2**.[5] Utilizing D-serine as the starting material and following the same route allowed synthetic elaboration of **3** and **4**. Diastereomeric purity

was examined via reverse phase HPLC analysis and enantiomeric purity was verified via chiral HPLC methods (see supporting information for details).

Inhibition of Stat5 phosphorylation by 1, 2, 3 and 4

With **1** and its three related stereoisomeric derivatives (**2**, **3** and **4**) in hand, we set out to ascertain each compounds ability to effectively inhibit Jak3. The Jak-Stat signaling pathway is a major regulatory element for gene transcription and plays a key role in processes such as immunoregulation and cellular proliferation and differentiation.[13] Jak3 natively associates with the common gamma chain γc forming a shared receptor for selected cytokines [including interleukin (IL)-2, IL-4, IL-7, IL-9, IL-15, and IL-21].[14] Upon cytokine binding, Jak3 is phosphorylated (presumably autophosphorylation), allowing signal transducers and activators of transcription (Stats) to bind to the cognate cytokine receptors via conserved Src homology 2 (SH2) domains.[15] Receptor-bound Stats are phosphorylated, dimerize (both homo and heterodimerization) and translocate to the nucleus to trigger gene transcription. To examine cellular Jak3 activity directly, we analyzed enriched, human CD4+ T cells isolated from PBMC's incubated with each compound at relevant concentrations (5 nM, 50 nM and 500 nM) and a DMSO control prior to stimulation with IL-2. The degree of Stat5 phosphorylation was analyzed from cell lysates via immunoblotting with an anti-phospho-Stat5 mAb (anti-actin mAb was performed as a control to confirm equal protein loading) (Figure 2, left blot). From this experiment it was clear that only CP-690,550 (**1**) maintained the ability to affect Stat5 phosphorylation at the concentrations tested, highly suggesting that the alternate stereochemical configurations of the molecule had deleterious effects on Jak3 inhibition.

IL-12 is another important immunoregulatory cytokine. The IL-12 receptor comprises two subunits that associate with Jak2 and Tyk2 and activates Stat4.[16,17] A primary selectivity issue for **1** is its reported downregulation of Jak2. We examined the ability of each compound to block the phosphorylation of Stat4 within IL-12 stimulated cells (Figure 2, right blot). The results demonstrate no clear inhibition by **1** or its related stereoisomers. This suggests that **1** (**1**) is capable of selectively inhibiting Jak3, without disrupting the functions of Jak2 or Tyk2 in a cellular environment at the concentrations tested.

Analysis of Kinase Selectivity

To fully understand these compounds potential, we pursued a direct analysis of each stereoisomer against purified Jak3. Further, **1** represents a novel and unique chemotype for kinase inhibition and it was of interest to profile each stereoisomer across a panel of kinases. Recently, Ambit Biosciences reported the aforementioned quantitative analysis of 38 known kinase inhibitors (including **1**) across a panel of 317 kinases.[9] We submitted **1** and the stereoisomeric analogues **2**, **3** and **4** across the same panel (at present containing 354 kinases). The initial profile provides activity as a percentage of DMSO control (for the full report see the supporting information section). Activities beyond a selected threshold were submitted for Kd determinations and the results are shown as a dendrogram representation in Figure 3. The profile of **1** closely matched the published data [with 2 notable exceptions: Mst2 – 'no hit' (reported IC50 of 4.2 μM) and Tyk2 – 'no hit' (reported IC50 of 620 nM)]. The profile additionally found a Kd of 210 nM for **1** at Rock (Rock was not part of the original 317 kinases screened in ref 9). Full Kd determinations for **1** were pursued for the 4 related Jak targets as well as the Jak1 (JH2domain-pseudokinase). These results confirmed that **1** binds Jak3 and Jak2 nearly equipotently (Kd of 0.75 nM for Jak3 and a Kd of 1.8 nM for Jak2). The disassociation constants for **1** at Jak1 and Tyk2 were recorded at 1.7 nM and 260 nM, respectively (as compared to the earlier report of 640 nM binding at Tyk2). No affinity was observed for **1** at the Jak1 (JH2domain-pseudokinase). These data contrast sharply with the original report denoting a higher degree of selectivity for Jak3 over Jak2 and Jak1. Interestingly,

these results conflict with the cell based study showing little or no inhibition of Stat4 phosphorylation by **1**.

The profile results for **2**, **3** and **4** indicate that each stereoisomer retains a degree of affinity for Jak3 and Jak2, though the potency of the interaction drops significantly. The profile for **3** (the enantiomer of **1**) showed solitary activity at Jak3 and Jak2 (Kd's of 180 nM and 270 nM, respectively). Enantiomers **2** and **4** had similar Kd's for Jak3 and Jak2, but also maintained several novel interactions. For instance, **2** was found to have modest binding potential for Mst1 and Mst2 (Kd's of 320 nM and 450 nM respectively). Analogue **4** was found to have modest binding at Map4K3 and Map4K5 (Kd's of 460 nM and 790 nM respectively). Mst and Map4K kinase subfamilies reside on the related STE20 and STE7 branches of the kinome. That enantiomers **2** and **4** show activity at these related targets suggests that this chemotype may represent a novel starting point for the development of selective inhibitors of these important kinase classes.

Minimum energy conformations of unbound 1, 2, 3 and 4 in water

Chirality, pharmacology and drug discovery are intertwining subjects dating back to the early use of quinine, atropine and opiates to today's blockbuster chiral drugs including Lipitor®, Zocor® and Pravachol®. In each instance, the chiral nature of these small molecules plays a role in their biochemical efficacy. With a deeper understanding of the chiral nature of **1** and its kinase selectivity profile we explored the role of the (4*R*)-methyl substituent and the (3*R*)-deazapurine moiety in defining its minimum energy conformation and how this probable conformation facilitates binding to Jak3.

The conformational space of the unbound inhibitors **1**-**4** was studied by subjecting the molecules to two consecutive Monte Carlo multiple minimum (MCMM) conformational searches (initially *in vacuo*, subsequently in implicit water). The resulting minimum energy models are shown in Figure 4 and can be discussed utilizing the truncated Fourier (TF) series-based coordinates for the description of six-member ring puckering established by Haasnoot[18] (plots representing the azimuthal θ angles, the two torsional angles describing the orientation of the base, and percentage energy increase of the various conformers obtained for **1**-**4** and are provided in the supporting information). The six-member ring of all the compounds can adopt two diametrically opposite chair conformations, represented by θ angles of 0° and 180°. Enantiomers **1** and **3**, which have the methyl substituent and the base on the same side of the ring plane, show a clear preference for having the methyl substituent in an equatorial position and the deazapurine moiety in an axial position (preferred θ of ~180° for **1** and ~0° for **3**). Enantiomers **2** and **4** position these substituents on opposing sides of the plane of the piperidine ring conferring a stronger preference for having the two substituents in equatorial positions (preferred θ of ~0° and ~180° for **2** and **4**, respectively). Interestingly, the signal for piperidine ring C3-H of **1** was noted at 4.78 ppm while the C3-H of **2** was found at 4.32 ppm (assigned via COSY analysis). The relative downfield shift in **1** highly suggests a more equatorial character for the C3-H of **1** and relative axial character for the C3-H of **2**, which is consistent with the results from the MCMM searches.

Using the deazapurine base as the anchor point for discussion (and likely for binding to Jak3) it is clear that even the fairly 'minor' change of the stereochemical configuration of the methyl group in structures **1** and **2** results in significant changes in the ultimate three-dimensional structures of these agents. This broadly accepted phenomenon is intensified when placing chiral substituents on five- and six-member ring structures due to hypersensitivity in ring conformations.

Docking of 1, 2, 3 and 4 at Jak3

There are 4 members of the Jak family of kinases; Jak1, Jak2, Jak3 and Tyrosine kinase 2 (Tyk2).[15] Each member of this family retains seven conserved sequence regions (or Jak homology domains); the JH1 domain (or kinase domain), the JH2 domain (or pseudokinase domain), the JH3 and JH4 domains (both are SH2 domains) and JH6 and JH7 (collectively the FERM domain or four-point-one, ezrin, radixin and moesin homology domain).[13,15] In 2005, Boggon et al. reported the crystal structure for the Jak3 kinase domain bound to the staurosporine analog AFN941.[19]

Utilizing this structure as a template, the four stereoisomers **1-4** were docked at the Jak3 catalytic cleft using Glide 4.5 in order to shed light on the mechanistic preference for the binding of **1**.[20] In particular, on the basis of the crystallographic coordinates of the Jak3 - AFN941 complex, the inhibitors were docked at the ATP-binding site, lined by residues from the N-terminal lobe on the roof of the pocket (Leu828, Gly829, Val836, and Ala853), the C-terminal lobe on the floor of the pocket (Leu956, Gly908, and Cys909), and the hinge region (from Met902 to Leu905). The opening of the cleft is defined by hydrophilic residues like Arg953, Asn954, Asp949 and Gln988. Interactions with residue backbones of the hinge region define the binding motif of many kinase inhibitors (including AFN941 with Jak3). We, therefore, utilized specified hydrogen bonds between Glu903 and Leu905 and each stereoisomer as a criterion for retrieving the ligand poses from the docking results along with the docking score and the energetic contributes to the binding interactions.

The results from the highest scoring Jak3-**1** docking complex are shown in Figure 5 and illustrate that the N1 and N7 nitrogens of the deazapurine moiety participate in key hydrogen bonds with residues Glu903 and Leu905. These interactions mimic hydrogen bonds found within the crystal structure of Jak3 with AFN941. Another significant interaction involves hydrogen bonds formed between the nitrile function and Arg953 at the opening of the cleft. This docking pose further validates the notion that the 4*R*-methyl group occupies an equatorial position while the 3*R*-base moiety is directed into an axial position in the chair conformation of the piperidine ring.

Comparing the docking poses for **1**, **2**, **3** and **4** found in the highest scoring Jak3 docking complexes to the minimum energy structures of the unbound **1**, **2**, **3** and **4** from the conformational analyses provides valuable insight into the superior binding associated with the (3*R*, 4*R*) stereochemical configuration of **1**. Figure 6 shows the predicted unbound conformation for each compound overlaid with the conformation associated with docking at Jak3. From this rendering, it is clear that only **1** docks with Jak3 in a conformation that extensively resembles the compounds minimum energy conformation (Figure 6a). For **2**, the six-member ring assumes a half-chair conformation with both the substituent in equatorial position (Figure 6b). Compound **3** docked with the six-member ring in a chair conformation and, contrary to the conformational preferences revealed by the MCMM search, the methyl and base substituents were found in the axial and equatorial position, respectively (Figure 6c). Finally, compound **4** docked with the six-member ring in a twist-boat conformation with both methyl and base substituents in the equatorial position (Figure 6d). These data indicate that compounds **2**, **3**, and **4** are forced to adopt unlikely high energy conformations in order to bind effectively at the Jak3 catalytic site.

Discussion

Inhibition of Jak3 and Jak2 by CP-690,550

Jak3 represents an intriguing therapeutic target.[21] Jak3 is primarily expressed within T cells and NK cells and specific mutations to Jak3 result in $T^{-}B^{+}NK^{-}$ severe combined

immunodeficiency (SCID).[22] Unsurprisingly, the knockout phenotype for Jak3 is a viable, but immunocompromised animal.[23] Conversely, Jak2 is ubiquitously expressed and knockouts are embryonic lethal.[24] Given these data, substantial effort has been invested in the search for highly selective Jak3 inhibitors.

Jak2 possesses a high degree of homology to Jak3 (47%) and is particularly homologous at the kinase active site.[19] Comparison between the catalytic pockets of crystal structures of Jak3 and Jak2 revealed conformational differences in the glycine rich loop and the activation loop that result in a rather tighter pocket for Jak2. Docking of **1** within the crystal structure of the catalytic cleft of Jak2[25] (see supporting information) suggests that the complexes of **1** with both Jak3 and Jak2 are decidedly similar. Only three residues in spatial proximity to the binding site of CP-690,550 at Jak3 and Jak2 are divergent: Jak3 Ala966 – Jak2 Gly993, in proximity of the DFG motif, Jak3 Cys909 – Jak2 Ser936, at the end of the hinge region, and Jak3 Gln988 – Jak2 Glu1015, in the activation loop. Cycles of MCMM conformational search performed on the Jak3- **1** complex granting flexibility to the ligand and the residues within a 4 Å radius allow for a potential hydrogen bond between the nitrile function and Gln988, an interaction that would be missing in Jak2. However, the docking pose of **1** in Jak2 does retain the key hydrogen bond with Arg980 (Arg953 in Jak3).

It is unclear how this lone deviation may affect binding, but given the relative Kd and IC_{50} values reported for **1** at both targets the difference is presumably negligible. This is also consistent with the fact that, due to the different conformation of the portion of the activation loop located immediately prior to the APE motif, in Jak2 Glu1015 points away from the binding site and would not be in proximity with the nitrile moiety.

From the docking comparisons, the similar disassociation constants for **1** at Jak3 and Jak2 are not surprising. Early results from the clinical use of **1** demonstrate efficacy, but also unwanted anemia and neutropenia.[26] This suggests that unwelcome downregulation of Jak2 is occurring to an appreciable extent. Nonetheless, phase 1 clinical evaluations demonstrated a reasonable safety profile and numerous phase 2 evaluations are currently underway. The IC_{50} values reported by Changelian et al. indicate a small degree of selectivity between Jak3 and Jak2. This data was collected via ELISA and is presumably more accurate than the Kd determinations presented here. Nonetheless, whether **1** binds/inhibits Jak2 at 1 nM or 20 nM concentrations, it is likely that the physiological levels of the drug will surpass the amount needed for effective downregulation of Jak2. The more compelling experiments, however, are cell based studies such as the assessment of inhibition of Stat4 phosphorylation by **1** (Figure 2) and the previous report that **1** effectively inhibits IL-2 stimulated cell proliferation (Jak3 dependent) while having much weaker effect on granulocyte macrophage-colony stimulation factor induced proliferation (Jak2 dependent). These results may provide tantalizing clues into the method by which cytokine receptor/Jak pairs initiate signaling cascades.

Conclusion

Kinases are among the most intriguing therapeutic targets in the human proteome and kinase inhibitors are becoming staples of the pharmacopeia. A primary doctrine of drug design is to limit the number of chiral centers placed into small molecules intended for clinical use for a myriad of reasons. **1** goes against convention and incorporates not one, but two chiral centers. Using a combination of molecular modeling, target profiling and cell-based analyses we have shown that the chiral nature of **1** is a key facet that defines its ability to bind and inhibit its primary target. Additionally, discrete stereoisomers of **1** may prove useful starting points for novel small molecules targeting alternate branches of the kinome. Finally, the divergence of activity for **1** in purified protein assays versus cell based assays remains an intriguing characteristic of this compound and should be explored further.

METHODS

Synthesis of 1, 2, 3 and 4

Complete procedures for the synthesis of **1**, **2**, **3** and **4** are presented in the supporting information section. The general strategy followed precedented chemistry from references 5, 11, and 12. Analysis of diastereopurity and enantiopurity were determined through reverse phase and chiral phase HPLC methods. Proton NMR for all enantiomers was identical. **3-((3*R*,4*R*)-3-((1H-Indol-4-yl)(methyl)amino)-4-methylpiperidin-1-yl)-3-oxopropanenitrile (1).** $[\alpha]_D$ ^{25}= +10.4 (*c* 0.64, MeOH); NMR spectra are complicated due to amide rotomers. ^{1}H NMR (400 MHz, $CDCl_3$) δ 12.67 and 12.63 (s, 1H), 8.39 and 8.37 (s, 1H), 7.40-7.44 (m, 1H), 6.80-6.90 (m, 1H), 4.78 (brs, 1H), 4.08-4.20 and 3.96-4.06 (m, 2H), 3.68-3.86 (m, 2H), 3.37-3.46 and 3.14-3.22 (m, 2H), 3.35 (s, 3H), 2.34-2.46 (m, 1H), 1.76-1.95 (m, 1H), 1.52-1.67 (m, 1H), 1.07 and 1.04 (d, *J*= 7.4 Hz, 3H); ^{13}C NMR (100 MHz, $CDCl_3$) δ 162.52, 162.46, 159.3, 159.0, 145.4, 145.1, 124.0 (br), 117.0, 116.9, 105.2, 104.9, 102.7, 56.8, 55.7, 45.2, 43.1, 42.1, 38.7, 35.8, 31.8, 31.4, 30.7, 25.8, 25.7, 14.4, 13.9; IR (neat) 3130, 2965, 1619, 1535, 1452, 1197, 1134, 1053, 906, 838, 720 cm^{-1}; HRMS (FAB) Calcd for $C_{16}H_{21}N_6O$ (M+H) 313.1777, found 313.1778. **3-((3*R*,4*S*)-3-((1H-Indol-4-yl)(methyl) amino)-4-methylpiperidin-1-yl)-3-oxopropane- nitrile (2).** $[\alpha]_D$ ^{25}= +74.8 (*c* 0.60, MeOH); The NMR are complicated due to the rotamers of the amide. ^{1}H NMR (400 MHz, $CDCl_3$) δ 12.58 (brs, 1H), 8.38 and 8.37 (s, 1H), 7.42 (s, 1H), 6.96 and 6.87 (d, *J*= 2.4 Hz, 1H), 4.32 (brs, 1H), 3.96-4.16 (m, 2H), 3.62-3.72 (m, 1H), 3.37 and 3.31 (s, 3H), 3.05-3.16 (m, 1H), 2.86-2.98 (m, 1H), 2.62-2.76 (m, 1H), 2.06-2.22 (m, 1H), 1.78-1.87 (m, 1H), 1.18-1.32 and 1.34-1.48 (m, 1H), 0.85 and 0.80 (d, *J*= 6.4 Hz, 3H); ^{13}C NMR (100 MHz, $CDCl_3$) δ 162.6, 162.4, 159.3, 159.0, 145.7 (br), 124.0 (br), 117.0, 116.9, 105.1, 104.7, 102.5 (br), 47.3, 46.1, 43.7, 42.5, 33.6, 33.0, 32.9, 25.9, 25.8, 18.5; IR (neat) 3123, 2963, 1599, 1541, 1452, 1198, 1137, 1056, 907, 830, 720 cm^{-1}; HRMS (FAB) Calcd for $C_{16}H_{21}N_6O$ (M+H) 313.1777, found 313.1775.

Profiles of 1, 2, 3 and 4

Kinase profiles were performed by Ambit Biosciences (San Diego, CA, USA: http://www.ambitbio.com/) utilizing KINOME*scan*™. Activity is recorded via a competition binding assay of selected kinases that are fused to a proprietary tag. Measurements of the amount of kinase bound to an immobilized, active-site directed ligand in the presence and absence of the test compound provide a % of DMSO control for binding of ligand. Activities between 0 and 10 were selected for Kd determinations. Dendrogram representations were generated by an in-house visualization tool designated PhyloChem. Dendrogram clustering and apexes are based on the human phylogenetic kinase data available at http://kinase.com/human/kinome.

Analysis of Stat5 and Stat4 phosphorylation

Human CD4+ positive cells were enriched from peripheral blood mononuclear cells obtained from a healthy donor by magnetic separation (CD4+ MACS beads). CD4+ cells were activated for 3 days with plate bound anti-CD3 and anti CD28 antibodies (5 ug/mL each), and then expanded for another 4 days in the presence of IL-2 (50 U/mL). Cells were rested overnight in 1% RPMI, and pre-incubated with **1**, **2**, **3**, **4** or DMSO control for 1 hour at indicated concentrations [(5 nM, 50 nM, 500 nM) DMSO concentration was equal in all preparations] and then activated with IL-2 (1000 u/ml) or IL-12 (100 ng/mL) for 15 minutes. Cells (10×10exp6/condition) were lysed in 1% Triton-x lysis buffer and equal amounts of cell lysate were run in NuPage Bis-Tris gel (4-12% gradient). Proteins were transferred onto nitrocellulose membrane. Detection was done with indicated antibodies using Odyssey western blotting system according to manufacturer's instructions.
[http://www.licor.com/bio/QuantitativeWesterns/index.jsp] Primary antibodies used: anti-actin mouse mAb (Chemicon), 1:5000, anti-phospho-Stat5 rabbit mAb (Cell Signaling), anti-

phospho-Stat4 (Zymed) 1:1000 and secondary goat-anti-mouse IgG Ab (Rockland) and goat-anti-rabbit IgG (Molecular Probes).

Monte Carlo conformational searches

Compounds **1-4** were sketched in Maestro and subjected to 100 steps of Monte Carlo Multiple Minimum (MCMM) conformational search performed *in vacuo* by means of MacroModel (Schrödinger, LLC, New York, NY, 2007).[27,28] The lowest energy conformer was subsequently used as the starting point for additional 1000 steps of MCMM search, this time performed using water as implicit solvent (Surface Generalized Born model). All calculations were conducted with the OPLS_2005 force field.

Protein preparation

The X-ray crystallographic structure of the human Jak3 kinase domain in a catalytically active state and in complex with the staurosporine derivative AFN941 was retrieved from the Protein Data Bank (PDB code: 1YVJ, atomic resolution 2.55 Å).[19] The protein structure was prepared for the docking studies using the Protein Preparation Wizard tool implemented in Maestro (Schrödinger, LLC, New York, NY, 2007). All crystallographic water molecules and other chemical components were deleted, the right bond orders were assigned and the hydrogen atoms were added to the protein. Arginine and lysine side chains were considered as cationic at the guanidine and ammonium groups, and the aspartic and glutamic residues were considered as anionic at the carboxylate groups. The hydrogen atoms were subsequently minimized employing the Polak-Ribiere Conjugate Gradient (PRCG) method until a convergence to the gradient threshold of 0.05 kJ/(mol Å). The atomic charges were computed using the OPLS_2005 force field.

Molecular Docking

All compounds were docked inside the active site of Jak3 using Glide 4.5,[20] the automated docking program implemented in the Schrödinger package (Schrödinger, LLC, New York, NY, 2007). The binding site was defined around the position occupied by the co-crystallized ligand in the Jak3 complex structure 1YVJ. In the Receptor Grid Generation a 10×10×10 $Å^3$ cubic docking box was generated and the known H-bond interactions between most of the kinase inhibitors and the backbone of the hinge segment were enforced defining the backbone amino groups of Leu905 and the backbone carboxylic groups of Glu903 as potential H-bond donor and acceptor respectively. The XP mode of Glide was utilized. The obtained complexes between Jak3 and the best scored pose of each compound were then submitted to 1000 steps of MCMM conformational search performed with the OPLS_2005 force field. The energy minimization was employed with PRCG procedure until convergence to the gradient threshold of 0.05 kJ/(mol Å). The reproduction of the binding mode of AFN941 in the catalytic site of Jak3 as in the crystallographic structure 1YVJ (RMSD value about 0.43 Å) validated the docking and MCMM search protocol used for this study.

Acknowledgements

We thank Dr. David Maloney and Dr. Douglas Auld for advice and help during the preparation of this manuscript. We thank Ms. Allison Peck for critical reading of this manuscript. This research was supported by the Molecular Libraries Initiative of the National Institutes of Health Roadmap for Medical Research, the Intramural Research Program of the National Human Genome Research Institute, the National Institute of Arthritis and Musculoskeletal and Skin Diseases and the National Institute of Diabetes and Digestive and Kidney Diseases, National Institutes of Health.

References

1. Changelian PS, Flanagan ME, Ball DJ, Kent CR, Magnuson KS, Martin WH, Rizzuti BJ, Sawyer PS, Perry BD, Brissette WH, McCurdy SP, Kudlacz EM, Conklyn MJ, Elliot EA, Koslov ER, Fisher MB, Strelevitz TJ, Yoon K, Whipple DA, Sun J, Munchhof MJ, Doty JL, Casavant JM, Blumenkopf TA, Hines M, Brown MF, Lillie BM, Subramanyam C, Shang-Poa C, Milici AJ, Beckius GE, Moyer JD, Su C, Woodworth TG, Gaweco AS, Beals CR, Littman BH, Fisher DA, Smith JF, Zagouras P, Magna HA, Saltarelli MJ, Johnson KS, Nelms LF, Des Etages SG, Hayes LS, Kawabata TT, Finco-Kent D, Baker DL, Larson M, Si M-S, Paniagua R, Higgins J, Holm B, Reitz B, Zhoa Y-J, Morris RE, O'Shea JJ, Borie DC. Prevention of Organ Allograft Rejection by a Specific Janus Kinase 3 Inhibitor. Science 2003;302:875–878. [PubMed: 14593182]
2. Blumenkopf TA, Flanagan ME, Munchhof MJ. EP 1234830, JP2003516405, US 2001053782, US6627754, WO0142246.
3. Hawkins JM, Makowski TM, Ruggeri SG, Rutherford JL, Urban FJ. JP 2007039455, WO 2007012953.
4. Flanagan ME, Li ZJ. JP 2005511696, US 2003130292, WO 03048162.
5. Cai W, Colony JL, Frost H, Hudspeth JP, Kendall PM, Krishnan AM, Makowski T, Mazur DJ, Phillips J, Ripin DHB, Ruggeri SG, Stearns JF, White TD. Investigation of Practical Routes for the Kilogram-Scale Production of cis-3-Methylamino-4-methylpiperidines. Org Process Res Dev 2005;9:51–56.
6. Sorbera LA, Serradell N, Bolós J, Rosa E, Bozzo J. CP-690,550. Drugs of the Future 2005;32:674–680.
7. Busque S, Leventhal J, Brennan D, Klintmalm G, Steinberg S, Shah T, Lawendy N, Wang C, Chan G. CP-690,550 (CP), a Jak3 Inhibitor, in De Novo Kidney Transplant (KT) Recipients: 6-month Results of a Phase 2 Trial. Am J Transplant 2007;(s2):304.
8. Kremer JM, Bloom BJ, Breedveld FC, Coombs J, Fletcher MP, Gruben D, Krishnaswami S, Burgos-Vargas R, Wilkinson B, Zerbini CAF, Zwillich SH. A randomized, double-blind, placebo-controlled trial of 3 dose levels of CP-690,550 versus placebo in the treatment of acute rheumatoid arthritis. 70th Annu Sci Meet Am Coll Rheumatol. 2007Abstract L40
9. Karaman MW, Herrgard S, Treiber DK, Gallant P, Atteridge CE, Campbell BT, Chan KW, Ciceri P, Davis MI, Edeen PT, Faraoni R, Floyd M, Hunt JP, Lockhart DJ, Milanov ZV, Morrison MJ, Pallares G, Patel HK, Pritchard S, Wodicka LM, Zarrinkar PP. A quantitative analysis of kinase inhibitor selectivity. Nat Biotechnol 2008;26:127–132. [PubMed: 18183025]
10. Changelian PS, Moshinsky D, Kuhn CF, Flanagan ME, Munchhof MJ, Harris TM, Doty JL, Sun J, Kent CR, Magnuson KS, Perregaux DG, Sawyer PS, Kudlacz EM. The specificity of Jak3 kinase inhibitors. Blood 2008;111:2155–2157. [PubMed: 18094329]
11. Hu XE, Kim NK, Ledoussal B. Synthesis of *trans*-(3*S*)-Amino-(4*R*)-alkyl-and –(4*S*)-Aryl-piperidines via Ring-Closing Metathesis Reaction. Org Lett 2002;4:4499–4502. [PubMed: 12465922]
12. Williams L, Zhang Z, Shao F, Carroll PJ, Joullié MM. Grignard Reactions to Chiral Oxazolidine Aldehydes. Tetrahedron 1996;52:11673–11694.
13. Yamaoka K, Saharinen P, Pesu M, Holt VET III, Silvennoinen O, O'Shea JJ. The Janus kinases (Jaks). Genome Biol 2004;5:253.1–253.6. [PubMed: 15575979]
14. O'Shea JJ, Park H, Pesu M, Borie D, Changelian P. New strategies for immunosuppression: interfering with cytokines by targeting the Jak/Stat pathway. Curr Opin Rheumatol 2005;17:305–311. [PubMed: 15838241]
15. Bhandari, R.; Kuriyan, J. Jak-Stat signaling. In: Bradshaw, R.; Dennis, E., editors. Handbook of Cell Signaling. Vol. 1. Academic Press; New York: 2003. p. 343-347.
16. Bacon CM, McVicar DW, Ortaldo JR, Rees RC, O'Shea JJ, Johnston JA. Interleukin 12 (IL12) Induces Tyrosine Phosphorylation of JAK2 and TYK2: Differential Use of Janus Family Tyrosine Kinases by IL-2 and IL-12. J Exp Med 1995;181:399–404. [PubMed: 7528775]
17. Bacon CM, Petricoin EF III, Ortaldo JR, Rees RC, Larner AC, Johnston JA, O'Shea JJ. Interleukin 12 induces tyrosine phosphorylation and activation of STAT4 in human lymphocytes. Proc Natl Acad Sci USA 1995;92:7307–7311. [PubMed: 7638186]
18. Haasnoot CAG. The Conformation of Six-Membered Rings Described by Puckering Coordinates Derived from Endocyclic Torsion Angles. J Am Chem Soc 1992;114:882–887.

19. Boggon TJ, Li Y, Manley PW, Eck MJ. Crystal Structure of the Jak3 kinase domain in complex with a staurosporine analog. Blood 2005;106:996–1002. [PubMed: 15831699]
20. Glide 4.5. Schrödinger, LLC; 2007.
21. Podder H, Kahan BD. Janus kinase 3: a novel target for selective transplant immunosuppression. Expert Opin Ther Targets 2004;8:613–629. [PubMed: 15584866]
22. Russell SM, Tayebi N, Nakajima H, Riedy MC, Roberts JL, Aman MJ, Migone T-S, Noguchi M, Markert L, Buckley RH, O'Shea JJ, Leonard WJ. Mutations of Jak3 in a Patient with SCID: Essential Role of Jak3 in Lymphoid Development. Science 1995;270:797–800. [PubMed: 7481768]
23. Thomis DC, Gurniak CB, Tivol E, Sharpe AH, Berg LJ. Defects in B lymphocyte maturation and T lymphocyte activation in mice lacking Jak3. Science 1995;270:794–797. [PubMed: 7481767]
24. Neubauer H, Cumano A, Muller M, Wu H, Huffstadt U, Pfeffer K. Jak2 deficiency defines an essential developmental check-point in definitive hematopoiesis. Cell 1998;93:397–409. [PubMed: 9590174]
25. Lucet IS, Fantino E, Styles M, Bamert R, Patel O, Broughton SE, Walter M, Burns CJ, Treutlein H, Qilks AF, Rossjohn J. The structural basis of Janus kinase 2 inhibition by a potent and specific pan-Janus kinase inhibitor. Blood 2006;107:176–183. [PubMed: 16174768]
26. Liu EH, Siegel RM, Harlan DM, O'Shea JJ. T cell-directed therapies: lessons learned and future prospects. Nature Immunol 2007;8:25–30. [PubMed: 17179969]
27. Chang G, Guida WC, Still WC. An Internal Coordinate Monte-Carlo Method for Searching Conformational Space. J Am Chem Soc 1998;111:4379–4386.
28. Mohamadi F, Richards NGJ, Guida WC, Liskamp R, Lipton M, Caufield C, Chang G, Hendrickson T, Still WC. Macromodel - An Integrated Software System for Modelling Organic and Bioorganic Molecules Using Molecular Mechanics. J Comput Chem 1990;11:440–467.

Abbreviations

Jak
Janus Kinase

Tyk
Tyrosine kinase

IL
interleukin

Stat
signal transducers and activators of transcription

MCMM
Monte Carlo multiple minimum

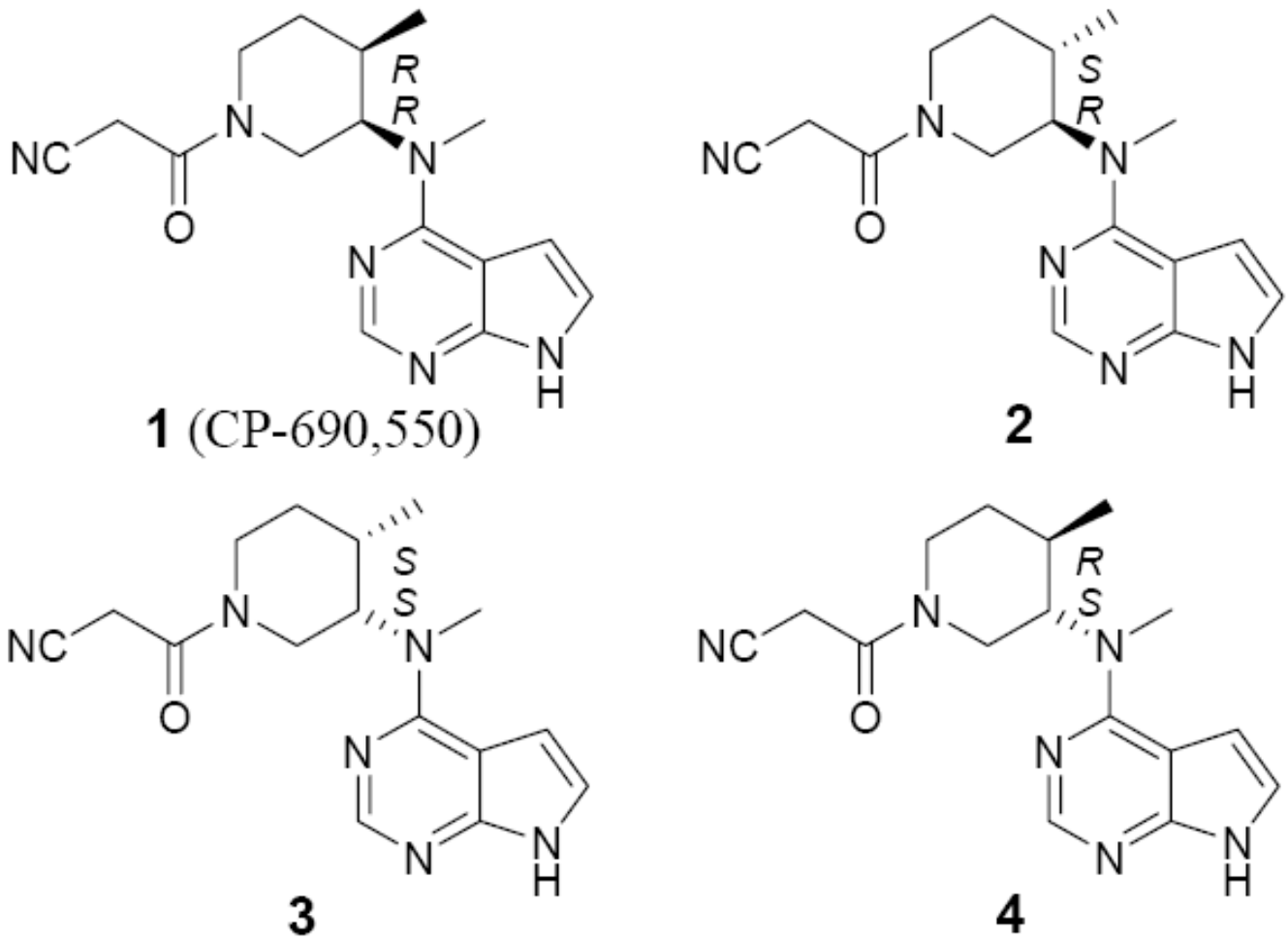

Figure 1.
The chemical structure of CP-690,550 (**1**) and related stereoisomers **2**, **3**, and **4**.

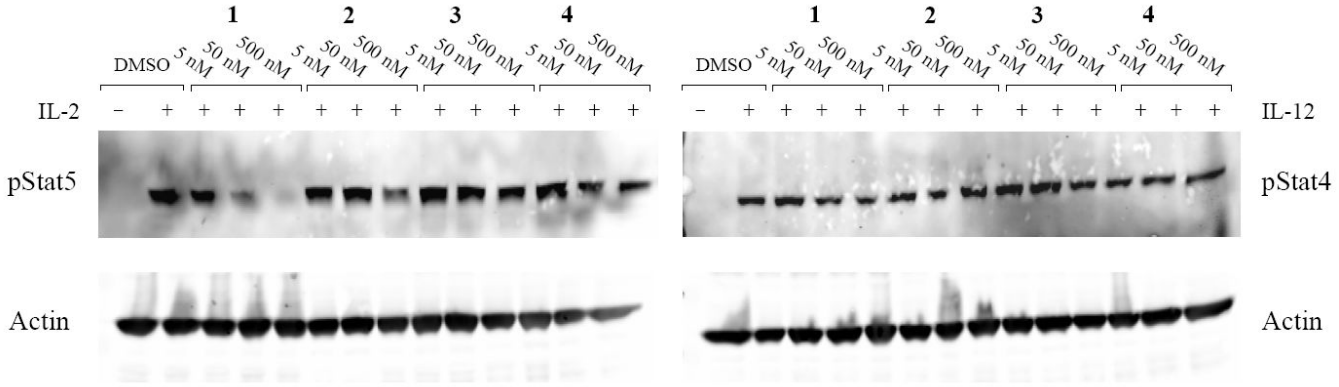

Figure 2.

Gel analysis showing the inhibitory ability of **1**, **2**, **3** and **4** to disrupt Stat5 phosphorylation (left blot) or Stat4 phosphorylation (right blot) in human CD4+ cells. CD4+ T cells were rested and incubated with DMSO control (lane 2), **1** (lane 3-5), **2** (lane 6-8), **3** (lane 9-11) or **4** (lane 12-14) at increasing concentrations (5 nM, 50 nM and 500 nM, respectively) for 1 h before being stimulated with IL-2 (1000 ug/mL; left blot) or IL-12 (100 ng/ml; right blot) for 15 minutes or incubated in medium without cytokine stimulation (lane 1; both gels). Cell lysates were partitioned, stripped and immunoblotted with anti-phospho-Stat5 (rabbit) mAb (left blot, top gel) or anti-phospho-Stat4 (rabbit) mAb (right blot, top gel). Anti-actin mAb (mouse) was used to confirm equal loading of protein across lanes (bottom gels).

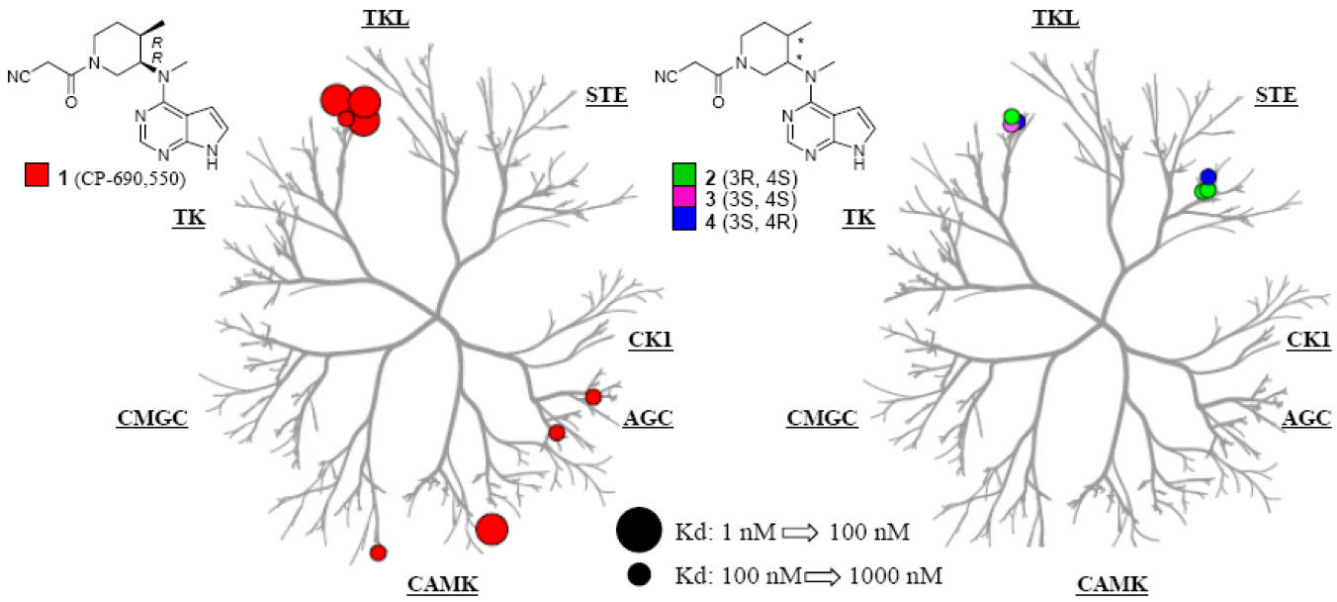

Figure 3.

Dendrogram representation of the selectivity profile for kinase inhibition by CP-690,550 (**1**) and stereoisomers **2**, **3** and **4** within a panel of 354 kinases. Activity for **1**: DCamKL3 = 4.5 nM, Jak1 = 3 nM, Jak2 = 2 nM, Jak3 = 0.7 nM, Tyc2 = 250 nM, Pkn1 = 200 nM, Snark = 420 nM, Tnk1 = 640 nM. Activity for **2**: Jak2 = 600 nM, Jak3 = 190 nM, Mst1 = 250 nM, Mst2 = 450 nM. Activity for **3**: Jak2 = 270 nM, Jak3 = 180 nM. Activity for **4**: Jak2 = 420 nM, Jak3 = 150 nM, Map4K3 = 460 nM, Map4K5 = 790 nM.

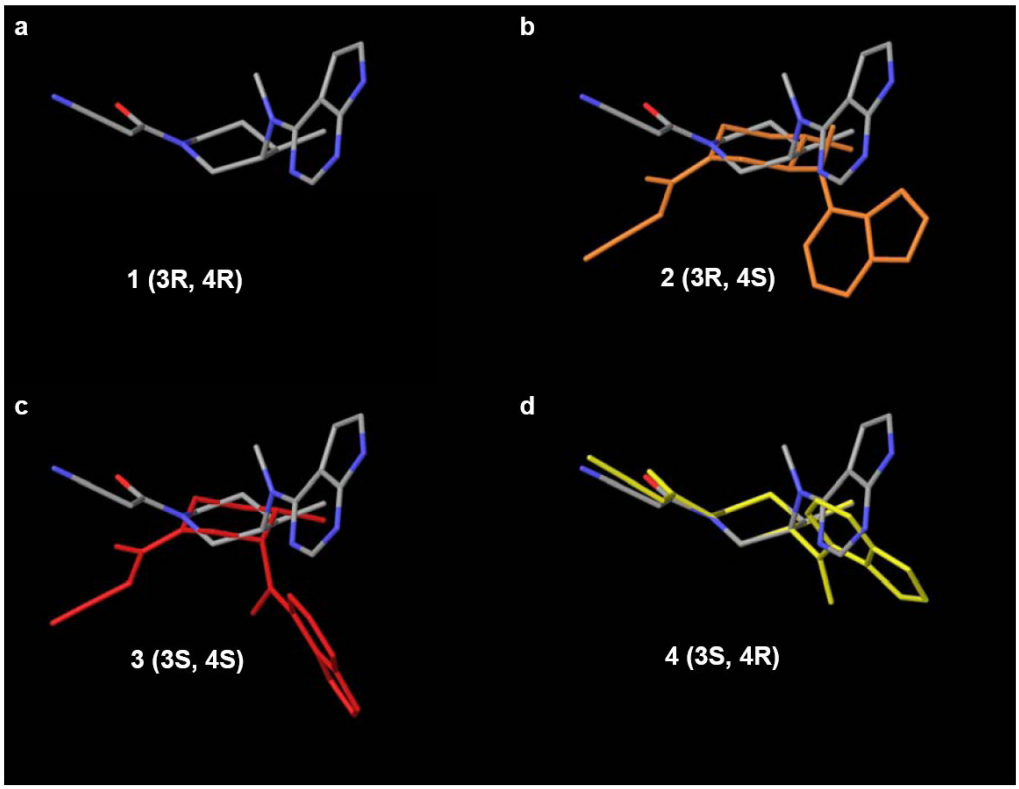

Figure 4.

Molecular models of the lowest energy conformers of **1**-**4** generated through Monte Carlo conformational searches. The model of **1** is colored by atom type (gray: carbon; red: oxygen; blue; nitrogen), while the models of **2**, **3**, and **4** are colored orange, red, and yellow respectively. Compounds **2**, **3**, and **4** are overlapped to **1** by superimposition of the six member ring atoms. All compounds prefer the chair conformation; however, **1** and **4** show a θ of ~180°, while **3** and **2** adopt the diametrically opposite chair conformation, with a θ of ~0°.

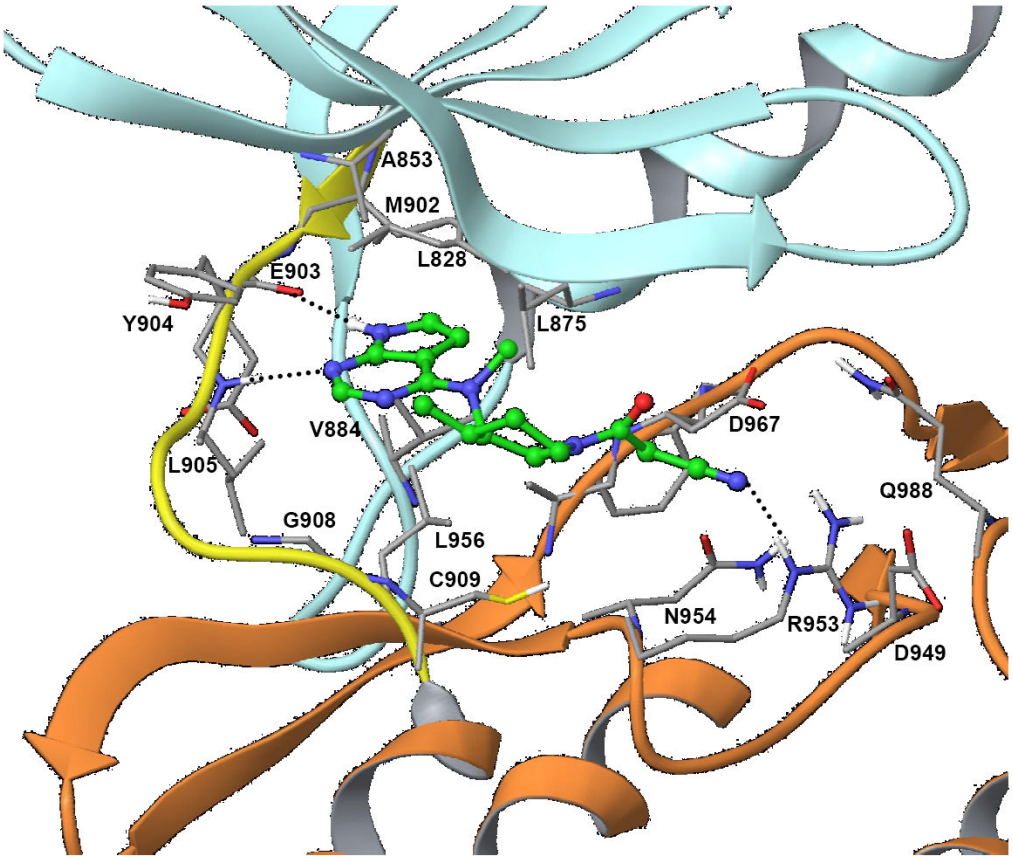

Figure 5.

Binding mode of **1** in the catalytic site of Jak3. The protein is shown with the ribbons representation with the N-lobe colored in cyan, the C-lobe in orange, and the hinge region in yellow. The residues in the binding pocket are colored by atom type. Compound **1** is shown as ball and stick model with carbon atoms colored in green. The major polar interactions between compound **1** and the residues in the pocket are highlighted as dotted lines.

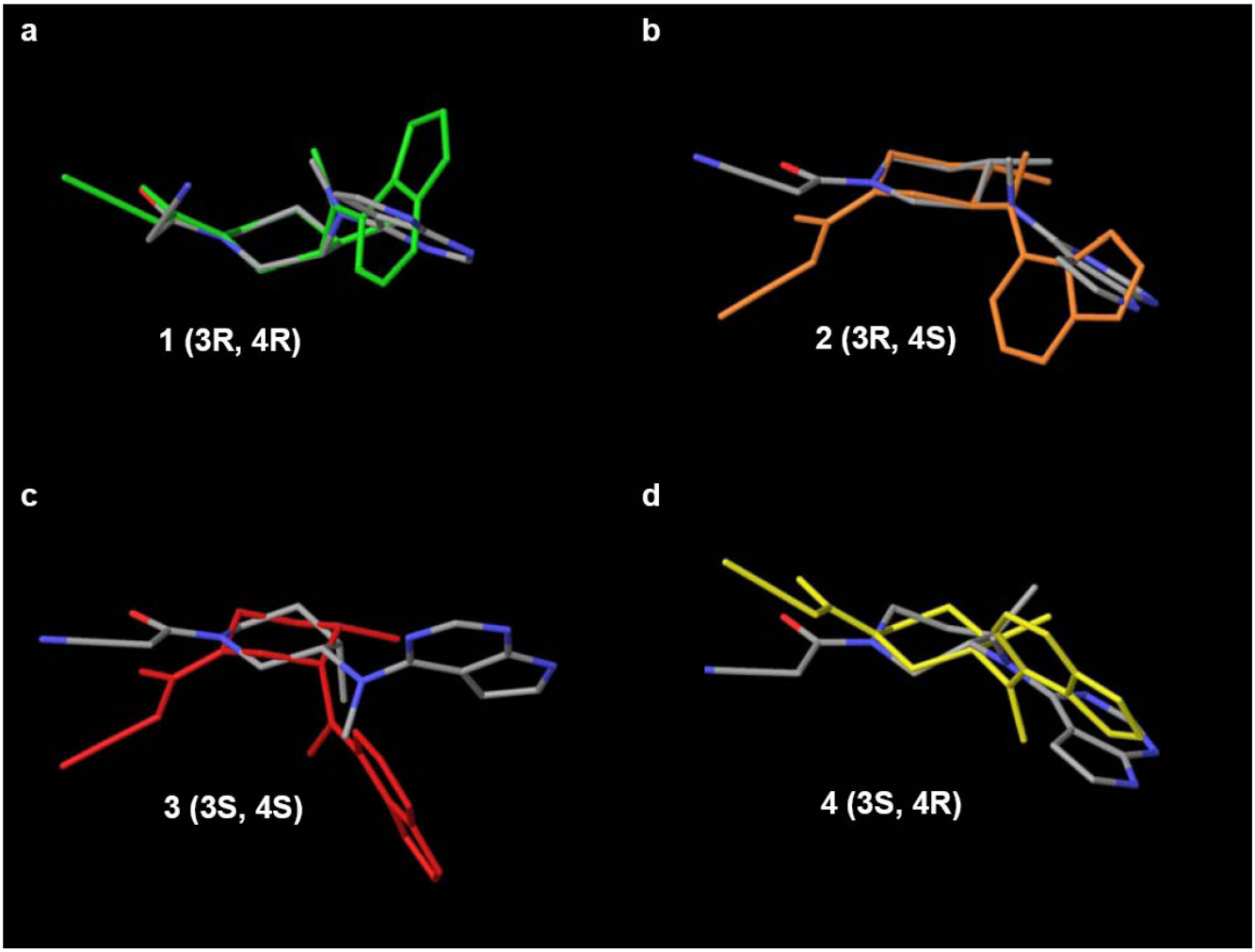

Figure 6.
Superposition of the six membered ring between the lowest energy conformation of compounds **1-4** (colored in green, orange, red, and yellow) and the respective best scored docking poses (colored by atom type).

Scheme 1.

Note: strategy and yeilds reflect those achieved and reported in *Org. Process Res. Dev.* **2005**, *9*, 51-56.

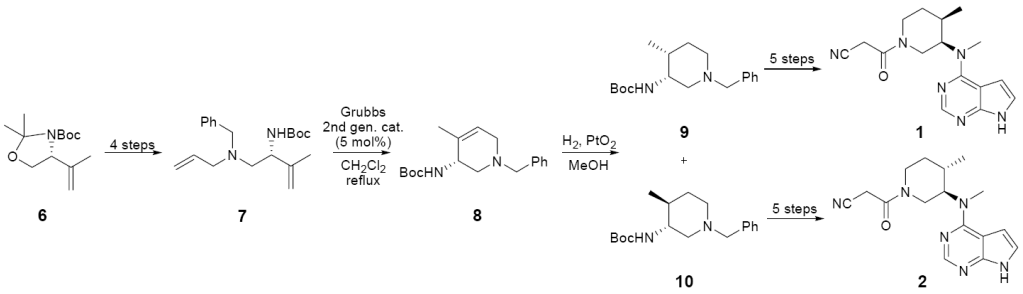

Scheme 2.